

## Anomalous Pressure-Induced Transition(s) in Ice XI

Koichiro Umemoto,<sup>1,2</sup> Renata M. Wentzcovitch,<sup>1,2</sup> Stefano Baroni,<sup>1</sup> and Stefano de Gironcoli<sup>1</sup>

<sup>1</sup>*SISSA—Scuola Internazionale Superiore di Studi Avanzati and INFM-DEMOCRITOS National Simulation Center, I-34014 Trieste, Italy*

<sup>2</sup>*Department of Chemical Engineering and Material Science and Minnesota Supercomputer Institute for Digital Simulation and Advanced Computation, University of Minnesota, Minneapolis, Minnesota 55455, USA*

(Received 23 May 2003; published 12 March 2004)

The effects of pressure on the structure of ice XI—an ordered form of the phase of ice *Ih*, which is known to amorphize under pressure—are investigated theoretically using density-functional theory. We find that pressure induces a mechanical instability, which is initiated by the softening of an acoustic phonon occurring at an incommensurate wavelength, followed by the collapse of the entire acoustic band and by the violation of the Born stability criteria. It is argued that phonon collapse may be a quite general feature of pressure-induced amorphization. The implications of our findings for the amorphization of ice *Ih* are also discussed.

DOI: 10.1103/PhysRevLett.92.105502

PACS numbers: 63.20.Dj, 64.70.Rh, 83.80.Nb

Ice *Ih* is the first system which was observed to amorphize under pressure [1]. It was soon argued that this behavior was related with the negative Clapeyron slope of the melting line of ice *Ih* and that amorphization would occur at the metastable extension of this line in the stability field of another high-pressure phase. By analogy, this idea led to the discovery of pressure-induced amorphization in silica—another icelike system [2]—as well as in several other materials [3]. More recently, careful calorimetric experiments in ice *Ih* have uncovered a more complex relationship between the amorphization phase boundary and the metastable extension of the melting line [4] of ice *Ih*. They both have negative Clapeyron slopes—a common feature of systems that undergo pressure-induced transitions to higher entropy forms—but these lines do not coincide. These experiments also indicated that the high-density amorphous and the frozen supercooled liquid differ at the atomic level, the former being an unrelaxed form of the latter [4].

Atomistic simulations related to amorphization [5,6] have helped to shed light into the atomic scale nature of this phenomenon, particularly in  $\alpha$ -quartz [7–10]. In spite of all the experimental and theoretical efforts devoted to pressure-induced amorphization, however, a solid and unified conceptual framework for understanding this phenomenon has not yet emerged [11], not even for two similar and relatively simple systems as quartz and ice. In this Letter, we address some of the questions that arise when trying to draw a parallel between amorphization in these two systems. We consider not ice *Ih*, but its hydrogen-ordered low-temperature form, ice XI. Amorphization in ice *Ih* occurs when the oxygen sublattice disorders and should not be much affected by the ordering state of hydrogen. Besides, being fully ordered ice XI should have more in common with silica. Here we investigate by first principles the mechanical and vibrational stability of ice XI under pressure, address the

effects of hydrogen disorder, and draw a parallel between our results and those previously obtained in  $\alpha$ -quartz.

The structure of ice *Ih* consists of a *hexagonal diamond* lattice of oxygen atoms with one hydrogen atom placed at random in one of the two energy minima existing in between every pair of oxygens, the overall symmetry being hexagonal ( $P6_3/mmc$ ). When the temperature is lowered below 72 K in the presence of small amounts of an alkali hydroxide [12] to facilitate nucleation, the hydrogen sublattice orders spontaneously, reducing the symmetry from hexagonal to orthorhombic ( $Cmc2_1$ ). The resulting ordered structure (ice XI; see Fig. 1) has four molecules per unit cell. Our calculations were performed within density-functional theory using the Perdew-Burke-Ernzerhof exchange-correlation functional [13] and the plane-wave pseudopotential method with

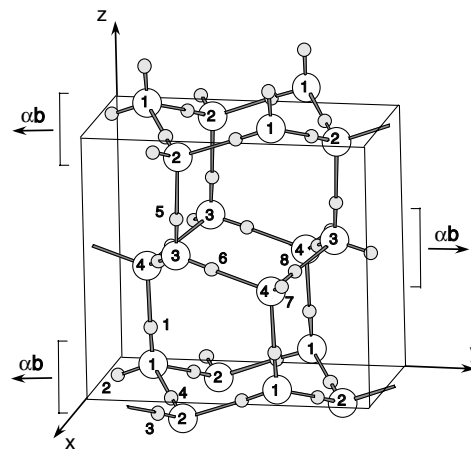


FIG. 1. Conventional cell of the base-centered orthorhombic structure of ice XI containing eight  $H_2O$  molecules. Gray and white circles denote oxygen and hydrogen atoms, respectively. The vector  $\alpha\mathbf{b}$  denotes the lateral displacement of layers which is allowed by symmetry and takes place under pressure (see text).

Troullier-Martins pseudopotentials [14]. Plane waves up to a kinetic-energy cutoff of 100 Ry were included in the basis set, corresponding to six  $k$  points in the irreducible Brillouin zone of the undistorted structure. Structural searches and optimizations under pressure were performed using damped variable cell shape molecular dynamics [15]. Phonon frequencies were calculated using density-functional perturbation theory [16,17], while elastic constants were obtained via the stress/strain relation using the stress tensor calculated quantum mechanically [18]. Calculations were done with the PWSCF package [19]. The structural parameters optimized at ambient pressure agree with experimental values [20,21] reasonably well (see Table I), the errors mainly affecting the longer OH bonds (on average 1.688 versus 1.774 Å [20]), while the shorter, intramolecular, bonds are on average better described (1.001 versus 0.981 Å [20]). The peaks' disposition in the translational and librational part of the vibrational density of states is similar to those measured experimentally [22,23]. However, the calculated frequencies [24] are approximately 20% larger. This is consistent with the calculated bulk modulus 40% larger and volume 6% smaller. These differences, which may be caused to a great extent by the neglect of quantum fluctuation effects, should not invalidate the phenomenology displayed in our study but should simply lead to an overestimation of the theoretical pressures.

The behavior of ice XI under pressure can be summarized as follows [24]: up to 33 kbar the lattice parameters decrease monotonically with the  $c$  parameter being slightly more compressible than the others. Adjacent layers parallel to the  $xy$  plane shift laterally with respect to each other along the  $y$  axis (see Fig. 1). The compression mechanism changes beyond 35 kbar. At this pressure the lattice parameter  $a$  starts increasing while the others decrease at a faster rate, particularly  $c$ . The hexagonal layers also displace at a faster rate. This behavior indicates the onset of an instability. Inspection of phonon

dispersions under pressure reveals the softening of the lowest transverse acoustic branch along the  $\Delta$  line [ $\mathbf{q} = (0, q, 0)$ ] (see Fig. 2). Around 15 kbar the frequency of the lowest acoustic mode at the  $Y$  point starts decreasing. As the pressure increases, the entire branch flattens and softens, until at 35 kbar the phonon frequency at  $\mathbf{q}^* \approx (0, \frac{4}{5}, 0)$  vanishes, and the entire acoustic branch goes soft (*collapses*) within a small pressure range. The vanishing of a single vibrational mode signals a mechanical instability towards a low-symmetry *ordered* phase which is commensurate or incommensurate with the original structure, according to whether  $(\mathbf{q}^* \cdot \boldsymbol{\tau})/2\pi$  is rational or not ( $\boldsymbol{\tau}$  being an integer translation of the Bravais lattice). When an entire portion of a vibrational branch softens simultaneously, many different incommensurate structures compete, thus giving rise to a *disordered* low-symmetry structure.

In order to investigate the nature of the interatomic arrangement resulting from this instability, we performed structural optimizations on a supercell commensurate with the wave vector of  $(0, \frac{4}{5}, 0)$  very close to the soft phonon  $\mathbf{q}^*$ . This supercell is 5 times longer along the  $y$  direction than the conventional orthorhombic cell, and thus it contains 40 molecules. We have started the optimizations from an atomic geometry where atoms were displaced from equilibrium along a pattern corresponding to the soft phonon. This mode is polarized parallel to the  $x$  axis. In the long wavelength limit it is equivalent to the shear strain  $\epsilon_6$ . Few configurations with different displacement amplitudes were optimized at 50 kbar. The resulting equilibrium geometry consists in an oxygen network where hexagonal atomic layers are laterally shifted with respect to each other along the  $y$  direction and modulated by the phonon wave number (see Fig. 3). The O—O pair distribution function does not change dramatically with respect to that of ice XI. The first coordination shell with four oxygen atoms widens and four oxygens from the second shell split off and approach

TABLE I. Lattice parameters and internal coordinates of ice XI. The numbers assigned to atoms are the same as in Fig. 1.  $H_1, H_2, H_3, O_1,$  and  $O_2$  are symmetrically equivalent to  $H_5, H_6, \{H_4, H_7, H_8\}, O_3,$  and  $O_4,$  respectively.

	$a$		$b$		$c$	
	Calc.	(Expt.)	Calc.	(Expt.)	Calc.	(Expt.)
	4.383	(4.4650) <sup>a</sup> (4.5019) <sup>b</sup>	7.623	(7.8590) <sup>a</sup> (7.7978) <sup>b</sup>	7.163	(7.2920) <sup>a</sup> (7.3280) <sup>b</sup>
	$x$		$y$		$z$	
$H_1$	0.0	(0.0) <sup>b</sup>	0.664	(0.6636) <sup>b</sup>	0.198	(0.1963) <sup>b</sup>
$H_2$	0.0	(0.0) <sup>b</sup>	0.541	(0.5363) <sup>b</sup>	0.017	(0.0183) <sup>b</sup>
$H_3$	0.683	(0.6766) <sup>b</sup>	-0.232	(-0.2252) <sup>b</sup>	-0.019	(-0.0183) <sup>b</sup>
$O_1$	0.0	(0.0) <sup>b</sup>	0.666	(0.6648) <sup>b</sup>	0.059	(0.0631)
$O_2$	0.5	(0.5) <sup>b</sup>	0.833	(0.8255) <sup>b</sup>	-0.066	(-0.0631) <sup>b</sup>

<sup>a</sup>Experimental data from Ref. [21].

<sup>b</sup>Experimental data from Ref. [20]

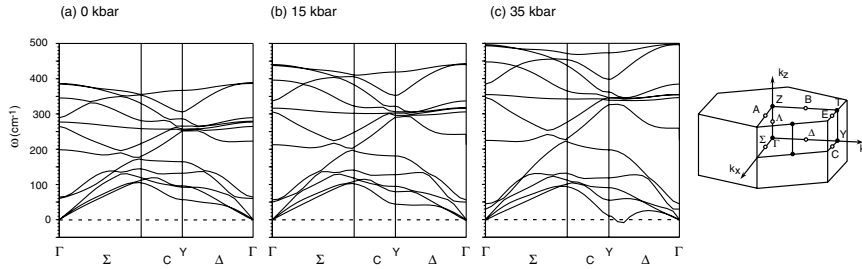


FIG. 2. Phonon dispersions of translational modes at 0, 15, and 35 kbar. Negative values correspond to imaginary frequencies. The Brillouin zone of the base-centered orthorhombic lattice is shown at the right.

the first one. However, no obvious bond reconstruction is observed [24]. Notice that ice VIII, the high-pressure phase stable at this pressure, has eight oxygen atoms in the first coordination shell. At 50 kbar, the density of ice VIII and of the modulated phase are 1.76 and 1.30 g/cm<sup>-3</sup>, respectively. At 30 kbar, right before the phonon collapse, the density of ice XI is 1.14 g/cm<sup>-3</sup>. Under decompression to 30 kbar, the modulated structure does not revert to the undistorted one. Several different initial configurations lead to the same final result, as long as the internal parameters are modulated by this wave number. This situation is typical of a first order phase transition, which is initiated by the softening of one mode and whose low-symmetry phase is separated by a finite energy barrier from the high-symmetry one.

The collapse of the acoustic branch implies an elastic instability that can be captured and expressed quantitatively through the Born stability criteria [25]. These criteria require that all the principal minors of the elastic constant tensor are positively defined. For an orthorhombic system these conditions expressed in the Voigt notation are

$$B_{1,ii} = c_{ii} > 0 \quad (i = 1-6), \quad (1)$$

$$B_{2,ij} = \begin{vmatrix} c_{ii} & c_{ij} \\ c_{ji} & c_{jj} \end{vmatrix} > 0 \quad (\{ij\} = \{23\}, \{31\}, \text{ or } \{12\}), \quad (2)$$

$$B_3 = \begin{vmatrix} c_{11} & c_{12} & c_{13} \\ c_{21} & c_{22} & c_{23} \\ c_{31} & c_{32} & c_{33} \end{vmatrix} > 0. \quad (3)$$

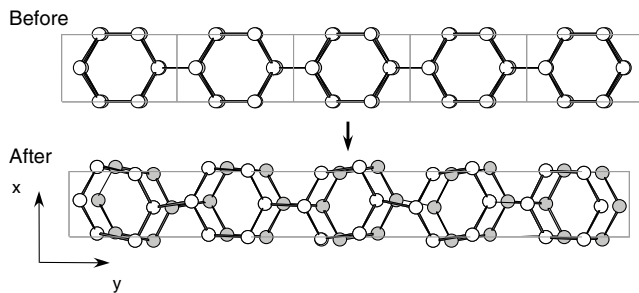


FIG. 3. Structural change from ice XI at 30 kbar to the modulated phase at 50 kbar commensurate with the reciprocal lattice vector (0, 4/5, 0). Gray and white circles denote oxygens on different layers. Hydrogens are omitted in this figure.

Figure 4 displays the behavior of these coefficients under pressure.  $B_{2,23}$ ,  $B_{2,31}$ , and  $B_3$  decrease rapidly beyond 25–30 kbar and approach zero around 40 kbar. This signals to the elastic instability associated with softening of the lowest transverse acoustic phonon branch that should occur if the incommensurate instability is inhibited. In ice *Ih*, molecular dynamics simulations with interatomic potentials have shown that some of the elastic moduli and Born coefficients decrease and approach zero at 9 kbar [5], a considerably lower pressure than we find here and similar to the amorphization pressure of ice *Ih* of 10 kbar [1]. Although the results of Ref. [5] cannot be directly compared to ours, because of the different theoretical and computational approaches followed in the two studies, we argue that it is reasonable that a proper account of hydrogen disorder would lower the transition pressure. Hydrogen disorder is responsible for the entropic stabilization of ice *Ih* at higher temperatures. Below 72 K, the relaxation of the larger number of structural degrees of freedom made available by hydrogen ordering further stabilizes ice XI. This lower enthalpy of ice XI will increase its pressure stability and metastability ranges as compared to ice *Ih*'s. Therefore, we conclude that ice XI should require higher pressure than ice *Ih* to amorphize.

Analogies exist between amorphization in ice and in  $\alpha$ -quartz. In the latter case, amorphization takes place between 21 and 30 GPa, in the stability field of stishovite [26]. Force-field simulations indicate [9] and first-principles calculations confirm [27] that pressure in this range softens an acoustic phonon mode at the *K*-point

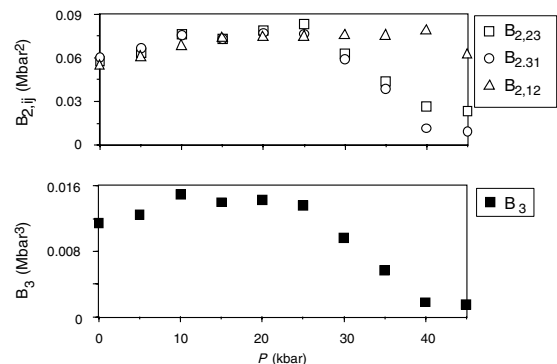


FIG. 4. Pressure dependence of the Born coefficients given by Eqs. (2) and (3).

zone edge. Indeed, an intermediate, commensurate, phase with an x-ray diffraction pattern which could result from the soft-phonon phase is found near 21 GPa [10,26]. This zone-edge instability happens to be related to an elastic instability [8] occurring at zone center. As a matter of fact, first-principles lattice-dynamical calculations [27] reveal that just before the softening of the  $K$ -point mode, the entire lowest acoustic branch along the  $T$  line starts flattening and collapses soon after the first instability at the zone edge. We argue that the amorphous state produced with increasing pressure and possibly under nonhydrostatic stresses, after the zone-edge instability, results from the competition between the several soft-phonon phases produced by the collapse of this acoustic branch.

Ice XI displays a similar phenomenology. According to ice's phase diagram [28], these instabilities should be taking place in the stability field of ice VIII, a robust high-pressure phase. Indeed, our calculations confirm that ice VIII is stable with respect to ice XI beyond 30 kbar, but several other intervening phases should be even more stable than ice XI at lower pressures. One difference with respect to  $\alpha$ -quartz, which might be irrelevant, is that the phonon instability starts at an incommensurate wave number. Several soft modes around  $\mathbf{q}^*$  should occur at pressures near 35 kbar. Nonhydrostaticity and higher pressures could result in instabilities at several wave numbers and finally along the entire  $\Delta$  line. This parallel between  $\alpha$ -quartz and ice XI strongly suggests the possibility of amorphization in ice XI, perhaps preceded by an incommensurate intermediate phase. Another difference with respect to  $\alpha$ -quartz that still needs to be further explored is the nature of the intermediate phase. The nearest neighbor environment in the intermediate phase of  $\alpha$ -quartz resembles more that in the stable high-pressure form, stishovite, than that in  $\alpha$ -quartz [10]. Silicon's coordination changes by means of a subtle mechanism from fourfold to fivefold and sixfold in the intermediate phase. Therefore, the intermediate phase seems to have a compromising high-coordination structure accessible in phase space. The potentially intermediate incommensurate phase we found in ice XI does not display any evident change in the nature of the crystal structure other than a modulation and a relative lateral displacement of the hexagonal layers, even though some structural rearrangement seems to be under way.

In summary, we have carried out a first-principles study of the vibrational and mechanical stability of ice XI under pressure. We have drawn a parallel with the behavior of ice *Ih* and of  $\alpha$ -quartz, systems that undergo pressure-induced amorphization. These comparisons suggest that ice XI will also amorphize, perhaps preceded by an incommensurate phase produced  $\approx$  35 kbar. Experimental work on the high-pressure behavior of ice XI would shed valuable light on the scenarios outlined in the present work, particularly in what concerns the ex-

istence and the role of the incommensurate phase which would be a precursor to amorphization.

S. B. thanks Paolo Giannozzi for his pristine interest in pressure-induced amorphization in silica and for the work done together on this subject. This research was supported by NSF Grants No. EAR-0135533 and No. EAR-0230319, by MIUR under the PRIN-2000 initiative, and by INFM through the MRC *Forum* project and *Iniziativa Trasversale Calcolo Parallelo*. Computations were performed at the Minnesota Supercomputing Institute and at the CINECA supercomputing center in Bologna.

- 
- [1] O. Mishima *et al.*, Nature (London) **310**, 393 (1984).
  - [2] R. J. Hemley *et al.*, Phys. Rev. Lett. **57**, 747 (1986).
  - [3] E. G. Ponyatovsky and O. I. Barkalov, Mater. Sci. Rep. **8**, 147 (1992).
  - [4] O. Mishima, Nature (London) **384**, 546 (1996).
  - [5] J. S. Tse, J. Chem. Phys. **96**, 5482 (1992).
  - [6] J. S. Tse and M. L. Klein, J. Chem. Phys. **92**, 3992 (1990).
  - [7] N. Binggeli and J. R. Chelikowsky, Phys. Rev. Lett. **69**, 2220 (1992).
  - [8] N. Binggeli *et al.*, Phys. Rev. B **49**, 3075 (1994).
  - [9] S. L. Chaplot and S. K. Sikka, Phys. Rev. Lett. **71**, 2674 (1993).
  - [10] R. M. Wentzcovitch *et al.*, Phys. Rev. Lett. **80**, 2149 (1998).
  - [11] E. Demiralp *et al.*, Phys. Rev. Lett. **82**, 1708 (1999); S. Chaplot, Phys. Rev. Lett. **83**, 3749 (1999); E. Gregoyanz *et al.*, Phys. Rev. Lett. **84**, 3117 (2000); M. H. Müser and P. Schöffel, Phys. Rev. Lett. **90**, 079701 (2003); E. Gregoyanz *et al.*, Phys. Rev. Lett. **90**, 079702 (2003).
  - [12] Y. Tajima *et al.*, Nature (London) **299**, 810 (1982).
  - [13] J. P. Perdew, K. Burke, and M. Ernzerhof, Phys. Rev. Lett. **77**, 3865 (1996).
  - [14] N. Troullier and J. L. Martins, Phys. Rev. B **43**, 1993 (1990).
  - [15] R. M. Wentzcovitch *et al.*, Phys. Rev. Lett. **70**, 3947 (1993).
  - [16] S. Baroni *et al.*, Phys. Rev. Lett. **58**, 1861 (1987).
  - [17] S. Baroni *et al.*, Rev. Mod. Phys. **73**, 515 (2001).
  - [18] O. H. Nielsen and R. M. Martin, Phys. Rev. B **32**, 3792 (1985).
  - [19] S. Baroni *et al.*, <http://www.pwscf.org>.
  - [20] A. J. Leadbetter *et al.*, J. Chem. Phys. **82**, 424 (1985).
  - [21] C. M. B. Line and R. W. Whitworth, J. Chem. Phys. **104**, 10008 (1996).
  - [22] J.-C. Li, J. Chem. Phys. **105**, 6733 (1996).
  - [23] S. Dong *et al.*, Chem. Phys. **270**, 309 (2001).
  - [24] K. Umemoto *et al.* (to be published).
  - [25] M. Born and K. Huang, *Dynamical Theory of Crystal Lattices* (Clarendon, Oxford, 1954).
  - [26] K. J. Kingma *et al.*, Science **259**, 666 (1993); K. J. Kingma *et al.*, Phys. Rev. Lett. **70**, 3927 (1993).
  - [27] S. Baroni and P. Giannozzi, in *High Pressure Materials Research*, edited by R. M. Wentzcovitch *et al.*, Mater. Res. Soc. Symp. Proc. No. 499 (Materials Research Society, Pittsburgh, 1998), p. 233.
  - [28] V. F. Petrenko and R. W. Whitworth, *Physics of Ice* (Oxford University, New York, 1998).